comments of Jacques Roovers are acknowledged with gratitude.

Registry No. Polybutadiene, 9003-17-2.

References and Notes

(1) (a) Current address: Exxon Chemical Co., Linden, NJ 07036. (b) Current address: Corporate Research Laboratories, Exxon Research and Engineering Co., Annandale, NJ 08801.
(2) Ferry, J. D. *Viscoelastic Properties of Polymers*, 3rd ed.; Wiley: New York, 1980.
(3) Graessley, W. W.; Shinbach, E. S. *J. Polym. Sci., Polym. Phys. Ed.* **1974**, *12*, 2047.
(4) Raju, V. R.; Menezes, E. V.; Marin, G.; Graessley, W. W.; Fetters, L. J. *Macromolecules* **1981**, *14*, 1668.
(5) Roovers, J.; Graessley, W. W. *Macromolecules* **1981**, *14*, 766.
(6) Pearson, D. S.; Helfand, E. *Macromolecules* **1984**, *17*, 888.
(7) Pearson, D. S. *Rubber Chem. Technol.* **1987**, *60*, 439.
(8) Doi, M.; Edwards, S. F. *The Theory of Polymer Dynamics*; Clarendon: Oxford, 1986.
(9) de Gennes, P.-G. *J. Phys. (Les Ulis, Fr.)* **1975**, *36*, 1199.
(10) Klein, J. *Macromolecules* **1978**, *11*, 852.
(11) Graessley, W. W. *Adv. Polym. Sci.* **1982**, *47*, 67.
(12) Bartels, C. R.; Crist, B.; Fetters, L. J.; Graessley, W. W. *Macromolecules* **1986**, *19*, 785.
(13) Struglinski, M. J.; Graessley, W. W. *Macromolecules* **1985**, *18*, 2630.
(14) Graessley, W. W.; Struglinski, M. J. *Macromolecules* **1986**, *19*, 1754.
(15) Berglund, C. A.; Carriere, C. J.; Ferry, J. D. *J. Rheol.* **1981**, *25*, 251.
(16) Graessley, W. W.; Raju, V. R. *J. Polym. Sci., Polym. Symp.* **1984**, *71*, 77.
(17) Hadjichristidis, N.; Roovers, J. *J. Polym. Sci.* **1985**, *26*, 1087.
(18) Roovers, J. *Macromolecules* **1987**, *20*, 148.
(19) Jacovic, M. S.; Pollock, D.; Porter, R. S. *J. Appl. Polym. Sci.* **1979**, *23*, 517.
(20) Dobrescu, V. *Polym. Bull.* **1981**, *5*, 75.
(21) Valenza, A. J.; LaMantia, F. P.; Acierno, D. *J. Rheol.* **1986**, *30*, 1085.
(22) Rochefort, W. E.; Smith, C. S.; Rachapudy, H.; Raju, V. R.; Graessley, W. W. *J. Polym. Sci., Polym. Phys. Ed.* **1979**, *17*, 1197.
(23) Young, R. N.; Quirk, R. P.; Fetters, L. J. *Adv. Polym. Sci.* **1984**, *56*, 1.
(24) Colby, R. H.; Fetters, L. J.; Graessley, W. W. *Macromolecules* **1987**, *20*, 2226.
(25) Hadjichristidis, N.; Xu, Z.; Fetters, L. J.; Roovers, J. *J. Polym. Sci., Polym. Phys. Ed.* **1982**, *20*, 743.
(26) Khasat, N.; Pennisi, R. W.; Hadjichristidis, N.; Fetters, L. J. *Macromolecules*, in press.
(27) Carella, J. M.; Gotro, J. T.; Graessley, W. W. *Macromolecules* **1986**, *19*, 659.
(28) Montfort, J. P.; Marin, G.; Monge, P. *Macromolecules* **1984**, *17*, 1551.
(29) Watanabe, H.; Sakamoto, T.; Kotaka, T. *Macromolecules* **1985**, *18*, 1436.
(30) Zimm, B. H.; Kilb, R. W. *J. Polym. Sci.* **1959**, *37*, 19.
(31) Klein, J. *Macromolecules* **1986**, *19*, 105.
(32) Fetters, L. J.; Kiss, A.; Pearson, D. S.; Quack, G.; Vitas, F. J., manuscript in preparation.
(33) Reference 2, p 231, eq 31.

Glass Transition and Melting Behavior of Poly(ethylene-2,6-naphthalenedicarboxylate)

Stephen Z. D. Cheng*† and Bernhard Wunderlich‡

Department of Chemistry, Rensselaer Polytechnic Institute, Troy, New York 12180-3590.
Received July 17, 1987

ABSTRACT: On the basis of thermal analysis the heat capacities of both solid (230–350 K) and liquid (390–600 K) poly(ethylene-2,6-naphthalenedicarboxylate) (PEN) have been established by measurements on over 30 samples. The heat capacity of the solid is structure-independent to 300 K. Between 300 and 390 K, a pre-glass transition increase in heat capacity is observed for the amorphous samples of the polymer. It contributes about 9.5 J/(K mol) to the heat capacity increase [80.1 J/(K mol)]. Above the glass transition temperature (390 K), poorly crystallized PEN shows a rigid-amorphous fraction (up to 0.2). The rigid-amorphous fraction starts to gain mobility at about 430 K and reaches zero after melting of the low melting fraction of the polymer. The glass transition temperature on cooling changes logarithmically (T_g = 382.3 + 2.03 ln q, q in K/min). The hysteresis of amorphous samples has been analyzed. The crystallization range was studied from 450 to 530 K by crystallizing on cooling from the melt and heating from the glass. Four types of crystallinities must be distinguished: w^c(H), w^c(M), w^c(L), and w^c(C), with fusion peaks at high, middle, and low temperatures. The last fraction, w^c(C), forms on cooling after crystallization and causes an increase in C_p starting at about 450 K. The metastability, sequence of crystallization, stepwise crystallization, and annealing phenomena are analyzed. The equilibrium melting parameters have been estimated to be $T_m°$ = 610 K, ΔH_f = 25 ± 2 kJ/mol, and ΔS_f = 41 ± 3.3 J/(K mol).

Introduction

Poly(ethylene-2,6-naphthalenedicarboxylate) (PEN) is a relatively well-known polymer used for engineering purposes. Most research on PEN has concentrated on photochemical properties, such as absorption,[1] fluorescence, and chemiluminescence.[2] A special property of PEN is the formation of liquid crystalline polymers when polymerized with suitable comonomers.[3]

The crystal structure of PEN was reported to be triclinic with dimensions of a = 0.651 nm, b = 0.575 nm, and c = 1.32 nm and angles of α = 81°21′, β = 144°00′, and γ = 100°00′.[4] Only brief reports for liquid-induced crystallization of PEN in dioxane, aniline, and methylene chloride were published.[5,6] A distinct spherulitic texture was found in these crystallizations, and their time and temperature dependence was also studied.[5,6] Infrared spectra of PEN have been reported several years ago.[7] A detailed thermal analysis of PEN has not been reported so far.

In this paper, we describe the thermal analysis of amorphous and various semicrystalline PEN samples. The solid and liquid heat capacities have been measured. Special attention has been paid to the temperature range between 300 K and T_g, where possible local molecular motion in the amorphous state causes an increase in heat capacity. A similar increase was found earlier for poly-

† Present address: Institute of Polymer Science, Department of Polymer Science, The University of Akron, Akron, OH 44325.
‡ Present address: Department of Chemistry, The University of Tennessee, Knoxville, TN 37996-1600.

0024-9297/88/2221-0789$01.50/0

ethylene (PE)[8] and poly(aryl ether ether ketone) (PEEK).[9] The knowledge of solid and liquid heat capacity data permits then the determination of the heat capacity increase, ΔC_p, at the glass transition temperature, T_g. The hysteresis at the glass transition and changes in ΔC_p with crystallization conditions will be reported.

PEN provides a new example of a polymer that may possess in the semicrystalline state a rigid-amorphous fraction. The rigid-amorphous fraction does not contribute to the increase in heat capacity at T_g and devitrifies only at higher temperature. Similar behavior was found in several polymers with phenylene groups in the main chain, for example, PEEK,[9] (poly(oxy-2,6-dimethyl-1,4-phenylene) (PPO),[10] and poly(thio-1,4-phenylene) (PPS).[11] The overall "rigid-fraction", f_r, is computed from C_p by setting

$$f_r = 1 - [\Delta C_p(m)/\Delta C_p(a)] \quad (1)$$

where $\Delta C_p(m)$ is the measured heat capacity increase at T_g for semicrystalline PEN and $\Delta C_p(a)$ applies to totally amorphous PEN. The crystallinity, in turn, is determined by

$$w^c = \Delta H_f(m)/\Delta H_f(c) \quad (2)$$

where $\Delta H_f(m)$ is the measured heat of fusion of the semicrystalline PEN and $\Delta H_f(c)$, the heat of fusion of 100% crystalline of PEN. If the crystallinity model (two-phase model) is valid, f_r is equal to w^c. If $f_r > w^c$, a rigid-amorphous fraction exists above T_g and can be quantitatively studied.

Finally, all semicrystalline PEN samples show below the main melting range premelting peaks as found frequently also in other polyesters.[12]

Experimental Section

Materials and Samples. The PEN for our research was kindly supplied by Prof. Guan of the Academy of Science, China. The intrinsic viscosity of the PEN at 298.2 K in phenol/o-dichlorobenzene (0.6/0.4) was 0.593 dL/g. The PEN was synthesized from 2,6-naphthalenedicarboxylic acid and diethylene glycol.

The PEN samples for differential scanning calorimetry (DSC) were enclosed in aluminum pans. The sample weights were over 15 mg in order to obtain sufficient sensitivity for heat capacity measurements. The precision of the sample weight was ±1 μg. The weights of empty pan, reference pan, and sample pan were controlled within ±2 μg.

Equipment and Experiments. All samples were measured with an updated computer-interfaced Perkin-Elmer DSC2 in our ATHAS Laboratory. The changes from the earlier system are as follows: The DSC's analog output was converted to a digital output by using a Nelson Analytical, Inc., Model 860 analog-to-digital interface and then fed into an IBM XT personal computer for data handling. The software was developed and installed by Laboratory Microsystems, Inc.

The A/D converter is a voltage-frequency converter. The output voltage of the DSC is converted to frequency in time intervals ranging from 20 μs to 9 s. Scan rate and sampling rate are specified by the user. In our heat capacity measurements the scan rate was 10 K/min and the sampling rate is 12 points/K. This leads to 120 points/min or 2 points/s. The length of the time interval of each voltage to frequency conversion is therefore 0.5 s. This technique permits a first averaging of the DSC output over the 0.5-s sampling time such that no information is lost. It is superior therefore to our prior A to D conversion technique where the data collection was interrupt-driven and most of the DSC signal did not contribute to the measurement.

The heat capacity runs were performed in four temperature ranges selected: from 220 to 360 K was the range of measurement for the solid heat capacity (below T_g); and 330 to 450 K, the glass transition was analyzed; the temperature range from 340 to 560 K permits the analysis of melting and that from 530 to 600 K is needed for the measurement of the heat capacity of the liquid.

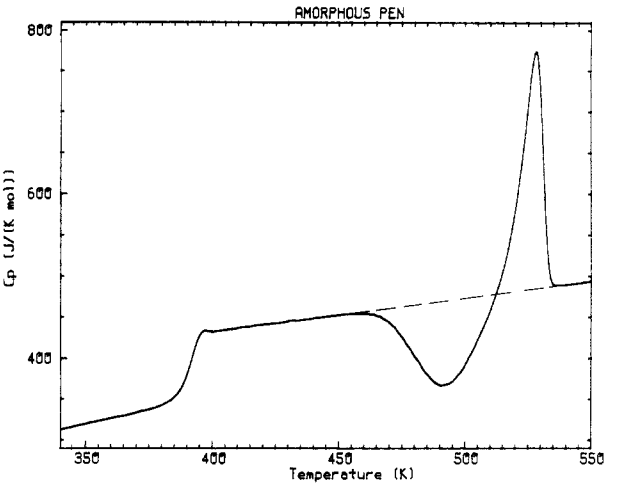

Figure 1. DSC melting trace of amorphous PEN. The sample was quenched from the melt to liquid N_2 temperature and measured at a heating rate of 10 K/min. The glass transition temperature, T_g, is 390 K; the heat capacity increase at T_g is 70.6 J/(K mol). (Note that the pre-glass transition increase in C_p cannot be analyzed without knowledge of the vibrational heat capacity. For details, see text.) Crystallization occurs from 460 to 510 K and melting from 510 to 540 K.

The DSC was calibrated in these four temperature ranges individually, following the standard procedures.[13] Both temperature and heat-flow scales were corrected by using standard materials. The repeatability of our Al_2O_3 heat capacity calibration was within ±0.1% based on the data of the National Bureau of Standards.[14]

A typical DSC melting trace of a liquid N_2 quenched PEN is shown in Figure 1. A fully amorphous PEN can be obtained since PEN crystallizes slowly as shown in the figure.

Isothermal crystallizations were carried out from the melt and the glass. For isothermal crystallization from the melt, the samples were first heated to 615 K and held for 2 min to destroy all crystalline nuclei. The samples were then cooled quickly to the prefixed crystallization temperature, T_c, and kept for the predetermined time, t_c. The isothermal crystallization was followed either by cooling at a rate of 10 K/min to 330 K, and subsequent analysis by heating, or by direct analysis from T_c without prior cooling. All DSC traces were recorded by using 10 K/min heating rate for the analyses. For the whole crystallization temperature range (450–530 K), crystallization occurs after an isothermal situation is reached.

For isothermal crystallization from the glassy state, the samples were heated to 615 K and held for 2 min, as before. The samples were then quenched in liquid N_2 to form the glass. Different crystallization temperatures, T_c, were chosen for isothermal crystallization, and the samples were heated from below T_g to T_c at the fastest DSC heating rate (320 K/min). The crystallization time, t_c, was counted from attainment of T_c. The same procedures as before (with and without prior cooling) were applied for the analyses.

In order to study the melting behavior, we used different heating rates (0.31–40 K/min) for the analysis of the samples crystallized isothermally (without cooling before analysis). Various partially crystallized samples were also measured in the temperature ranges of 220–360 K and 330–450 K.

Two-step isothermal crystallization experiments were carried out to get information on multiple melting peaks. The first step was partial crystallization at a lower temperature for a given time, to be followed by annealing or crystallization at a higher temperature. The second temperature was chosen where the lower melting peak had been observed before, usually 20 K above the lower crystallization temperature. A DSC melting trace was then recorded for analysis after the samples were cooled to 330 K with 10 K/min.

The glass transition regions were characterized by five temperatures, as before.[9-11] The first perceptible beginning of the glass transition, T_b, is judged by the initial increase in heat capacity from that of the solid state (glassy or crystalline). The extrapolated beginning and end of the glass transition are expressed

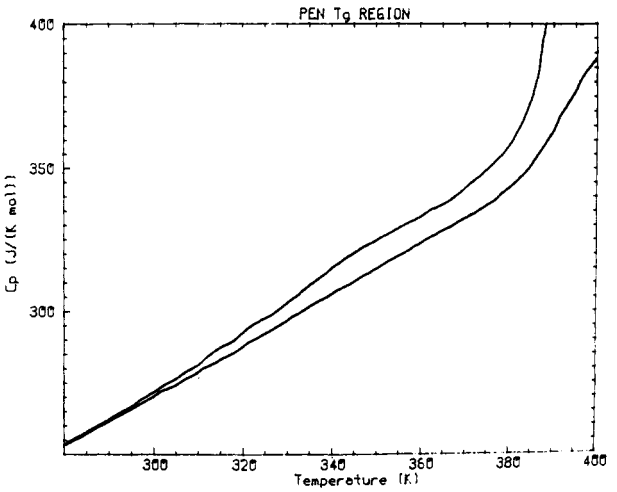

Figure 2. Difference of C_p below the glass transition temperature between the totally amorphous (upper curve) and a 0.54 rigid fraction sample of PEN (lower curve).

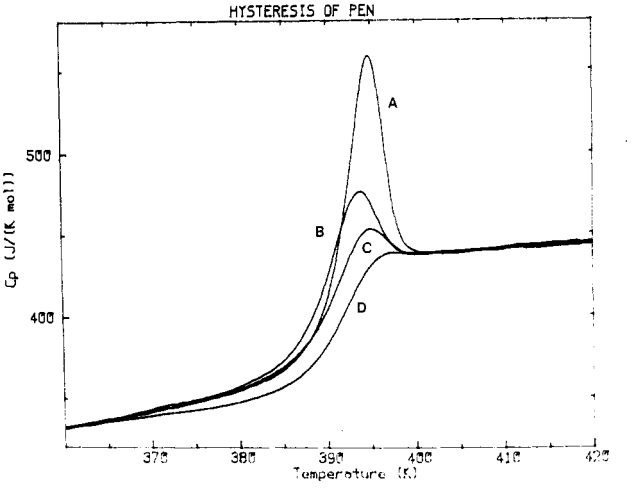

Figure 3. Hysteresis in heat capacity of amorphous PEN in the glass transition region at different cooling rates: (A) 0.31 K/min; (B) 2.5 K/min; (C) 10 K/min; and (D) quenched in liquid N_2 before heating at 10 K/min.

by T_1 and T_2 and are indicative of the broadeness of the major portion of the glass transition. The glass transition temperature, T_g, is chosen at half-devitrification when judged by the heat capacity increase. Finally, T_e, the end of glass transition, is reached when the heat capacity matches the liquid heat capacity. In case of hysteresis at the glass transition, the peak temperature and the heat of the hysteresis peak are also recorded (as the integration of C_p above the liquid base line with respect to temperature.

Finally, every sample was used only once for isothermal crystallization either from the melt or from the glass in order to minimize deterioration of the sample by cross-linking.

Results

Solid-State Heat Capacities of PEN. The experimental temperature range for the solid heat capacity measurements was 230–350 K. Similar to the situations of PEEK,[9] a small rigid fraction dependence of the heat capacity can be found even below T_g. Above 300 K (note that this is 90 K below T_g!) a difference between amorphous and semicrystalline PEN, which has the highest rigid fraction of 0.54, is seen. Amorphous PEN has a somewhat higher heat capacity. A gradual increase of this difference is seen up to about 340 K. After that, the difference is constant at about 3%, or 9–10 J/(K mol) as shown in Figure 2. Below 300 K, the heat capacity of amorphous PEN is practically identical with that of semicrystalline PEN.

The experimental measurements of semicrystalline PEN samples (18 runs) and of amorphous PEN samples (5 runs) were carried out in the temperature range 220–350 K. Below 300 K, all the solid heat capacity data were fitted into the equation

$$C_p = 0.0001616T^2 + 0.7544T + 29.256 \quad (3)$$

in J/(K mol) with a RMS deviation of ±0.8%. The experimental data have been used successfully in our solid heat capacity calculations, based on the independently determined group vibrational modes.[16] Surprisingly, the calculated solid heat capacity data fit our semicrystalline heat capacities measured below T_g (the curve of 0.54 rigid fraction in Figure 2). This may mean that the rigid-fraction dependence of heat capacity below T_g begins only below crystallinities of 50%. Since, however, in this temperature range C_p to C_v conversion is still not based on experimental expansivity and compressibility data, this observation must be taken as preliminary.

Liquid Heat Capacities and Glass Transition of Amorphous PEN. Two relatively wide temperature regions can be used for the measurement of the heat capacity of liquid PEN. The low-temperature range of about 40 K width, as shown in Figure 1, starts at the end of the glass transition (~405 K) and is limited by the crystallization exotherm that begins at about 450 K. The temperature range of 540–600 K is the second region to determine the liquid heat capacity. Because supercooling is needed for crystal nucleation,[15] this second set of measurements can be started somewhat below the melting temperature after cooling from the melt. A linear relationship between heat capacities and temperature was, as usual, found. It fits the following equation (RMS deviation ±0.8%)

$$C_p = 0.40941T + 268.35 \quad (4)$$

in J/(K mol) with 15 runs on 15 samples in both temperature ranges.

Combining the liquid heat capacity with the calculated solid state heat capacity data of PEN,[16] the heat capacity increase at the glass transition temperature is 80.1 J/(K mol) (T_g = 390 K, quenched PEN samples at a heating rate of 10 K/min). Curve D of Figure 3 shows the experimental ΔC_p of quenched PEN which is 70.6 J/(K mol) if the starting temperature of the glass transition region is taken to be 360 K. Adding the 9.5 J/(K mol) deviation below the glass transition shown in Figure 2 reaches the calculated value. A detailed report of thermodynamic functions of PEN will be given at a later date.[17]

Hysteresis in the T_g Region. Figure 3 shows the hysteresis of the heat capacity of quenched PEN in the glass transition region. The biggest hysteresis peak is Δh = 421 J/mol after the slowest cooling through the T_g region (curve A in Figure 3). The endotherm hysteresis peak decreases with increasing cooling rate, and the relationship between Δh and logarithmic cooling rate is shown in Figure 4. The data deviated from a straight line above cooling rates of 2.5 K/min, similar to the case of poly(oxy-2,6-dimethyl-1,4-phenylene) (PPO).[10] The quenched PEN samples show a small, but noticeable exothermic hysteresis peak at 380 K with Δh = −75 J/mol in curve D of Figure 3.

By integration of C_p from the glassy state to the equilibrium liquid the relative enthalpy of the glass can be established, and this, in turn, permits the evaluation what the temperature of the glass transition had been on cooling. Figure 5 shows the change of the glass transition as a function of cooling rate (q in K/min)

$$T_g = 382.3 + 2.03 \ln q$$

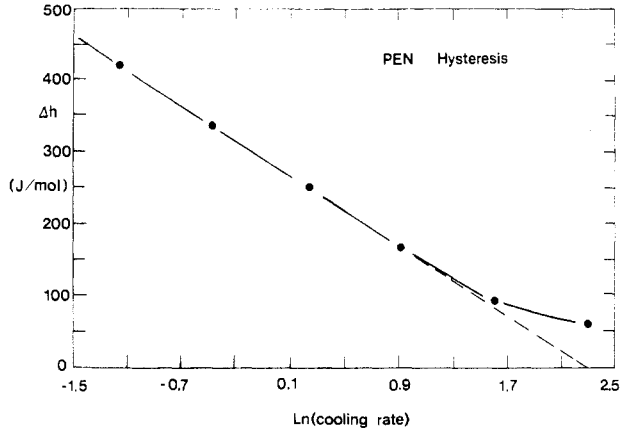

Figure 4. Relationship between the enthalpy under the hysteresis peak and the logarithm of the cooling rate for amorphous PEN. Heating rate is 10 K/min (ln 10 = 2.30).

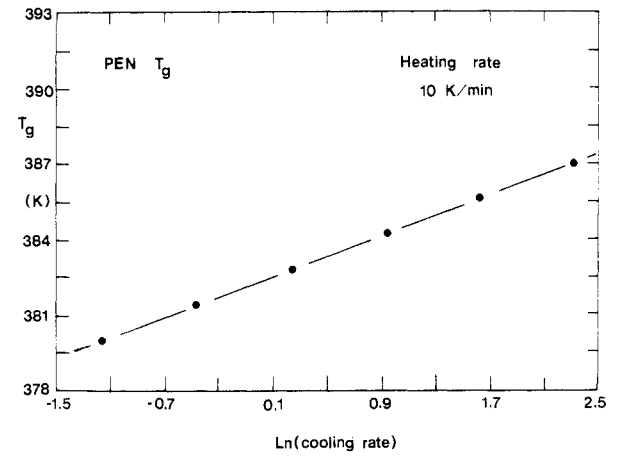

Figure 5. Relationship between T_g of amorphous PEN and the logarithmic cooling rate after the correction for the hysteresis effect (see text for details).

Glass Transition of Semicrystalline PEN. Table I shows the thermal properties in the glass transition region for 18 semicrystalline samples of PEN of different thermal histories. For isothermal crystallization from the melt the glass transition temperature, T_g, decreases with increasing crystallization temperature, T_c, up to 490 K. Further increase of T_c leads to an almost constant T_g of 387 K. Figure 6 shows the relationship between T_g and T_c of semicrystalline PEN crystallized from the melt. A similar relationship exists also for isothermal crystallization from the glassy state and is also shown in Figure 6. Other parameters in the T_g region show that the beginning of the glass transition, T_b, is practically constant (360 K), and T_1 decreases only by 1–2 K with increasing T_c. T_2 has the same tendency as T_g, and finally, T_e decreases continuously with increasing T_c. The combined data lead to a decrease of ΔT_1 up to T_c = 490 K and progressive decrease of T_2 in the whole T_c range we studied.

Heat Capacity of Semicrystalline PEN above T_g. Knowledge of the solid and liquid heat capacities allows the calculation of the rigid fraction between the glass transition, T_g, and the melting transition, T_m. Figure 7 shows the rigid-fraction dependence of the heat capacity above T_g. The solid lines were calculated from the known solid and liquid heat capacity data and the rigid fraction of eq 1. The solid circles are the experimental data of isothermal crystallization at T_c above 500 K that show no rigid-amorphous fractions ($f_r = w^c$). The open circles refer to T_c below 490 K, i.e., with various rigid-amorphous fractions (see Table II, below). For the solid circles, the experimental data fit the calculated data well up to 450 K. Above 450 K, however, a first positive deviation can be seen. This increase continues smoothly into the melting peak and indicates that the melting range is about 160 K wide. For the open circles, on the other hand, an increasingly positive deviation is observed starting about 20 K earlier, at 430 K.

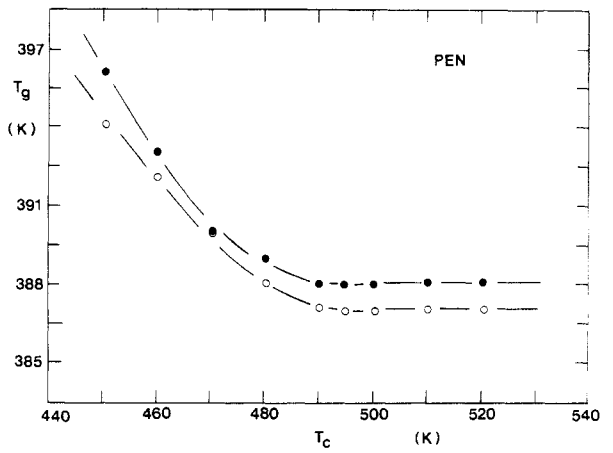

Figure 6. Relationship between glass transition temperature, T_g, and isothermal crystallization temperature, T_c, for both PEN crystallized from the melt (○) and the glass (●).

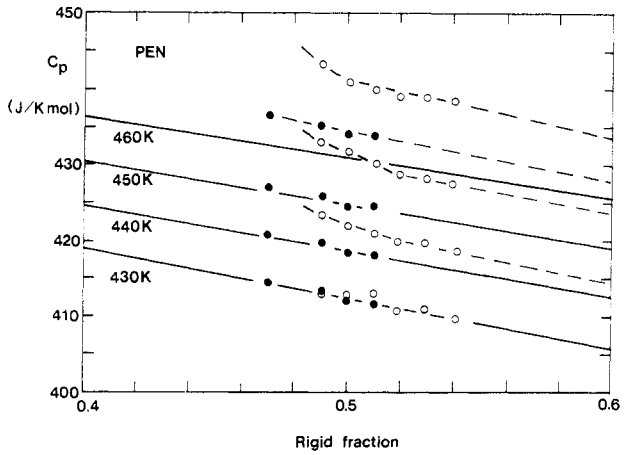

Figure 7. Rigid fraction dependence of the heat capacity above T_g. Solid lines are calculated on the basis of the solid and liquid heat capacities (see also ref 16 and 17). Points are experimental data: solid circles, isothermal crystallization above 500 K; open circles, isothermal crystallization below 490 K.

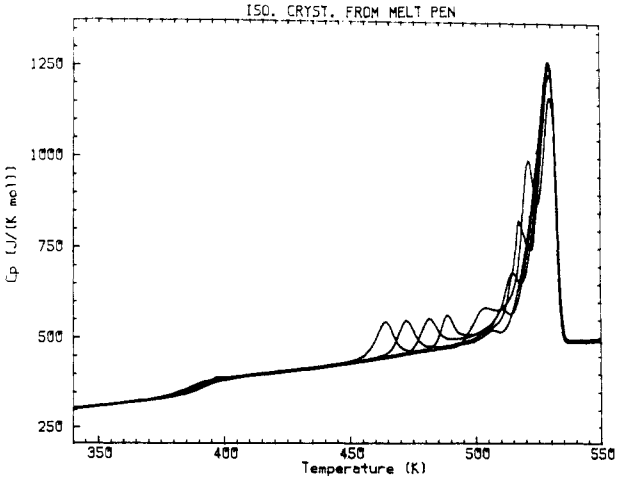

Figure 8. DSC melting traces of isothermal crystallization from the melt of PEN at 450, 460, 470, 480, and 490 K (for low-temperature melting peaks from left to right, respectively).

Table I
Thermal Properties of PEN in the Glass Transition Region Measured on Heating at 10 K/min

T_c and t_c	T_b (K)	T_1 (K)	T_g (K)	T_2 (K)	T_e (K)	$\Delta T_1{}^a$ (K)	$\Delta T_2{}^b$ (K)	ΔC_p [J/(K mol)]	f_r
A. Isothermal Crystallization from the Melt and Then Cooling at 10 K/min									
450 K, 2 h	360	380	394	409	435	29	75	42.3	0.49
460 K, 1.5 h	360	380	392	403	430	23	70	41.5	0.50
470 K, 1 h	360	380	390	398	425	18	65	40.7	0.51
480 K, 0.5 h	360	378	388	397	420	19	60	40.5	0.51
490 K, 1 h	360	378	387	396	415	18	55	38.2	0.54
495 K, 1.5 h	360	378	387	397	415	19	55	39.8	0.52
500 K, 2 h	360	378	387	396	413	18	53	40.6	0.51
510 K, 4 h	360	378	387	397	410	19	50	42.3	0.49
520 K, 15 h	360	378	387	397	405	19	45	40.3	0.51
B. Isothermal Crystallization from the Glass and Then Cooling at 10 K/min									
450 K, 2 h	360	380	396	410	435	30	75	42.5	0.49
460 K, 1.5 h	360	380	393	405	430	25	70	41.2	0.50
470 K, 1.0 h	360	380	390	400	425	20	65	40.4	0.51
480 K, 0.5 h	360	380	389	398	420	18	60	40.0	0.52
490 K, 1 h	360	379	388	397	415	18	55	38.6	0.53
495 K, 1.5 h	360	379	388	397	414	18	54	40.8	0.51
500 K, 2 h	360	379	388	397	413	18	53	42.2	0.49
510 K, 4 h	360	379	388	397	412	18	52	43.6	0.47
520 K, 15 h	360	378	388	397	410	19	50	41.7	0.50

$^a \Delta T_1 = T_2 - T_1$. $^b \Delta T_2 = T_e - T_b$.

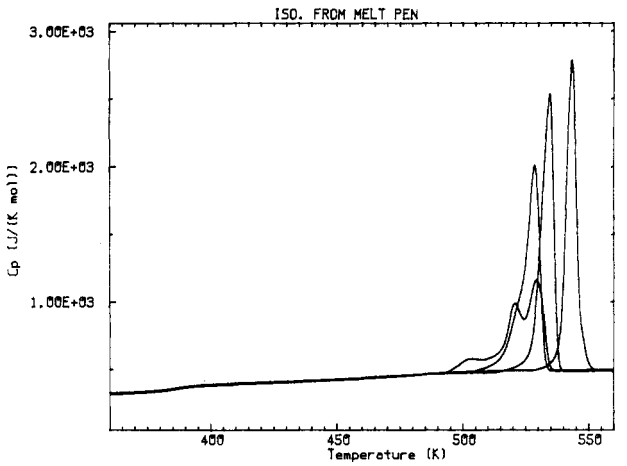

Figure 9. DSC melting traces of isothermal crystallization from the melt of PEN at 490, 500, 510, and 520 K (for melting peaks left to right, respectively).

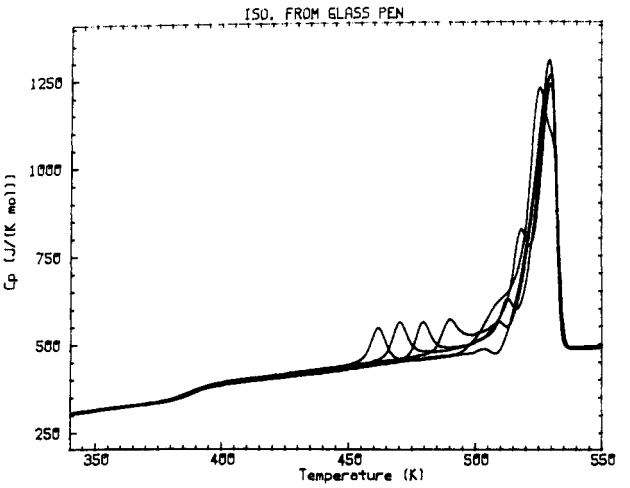

Figure 10. DSC melting traces of isothermal crystallization from the glass of PEN at 450, 460, 470, 480, and 490 K (for low-temperature melting peaks from left to right, respectively).

The lowest heat capacity above the low melting peak at T_c = 450 K is close to the liquid heat capacities.

Relationship between T_m and T_c. Figures 8–10 show DSC melting traces of semicrystalline PEN crystallized isothermally at different temperatures. For T_c = 490 K, three melting peaks can be characterized (Figure 8, see also Figure 11). The lowest, small melting peak occurs about 10–15 K above the crystallization temperature. The highest, large melting peak can be observed around 525–530 K with very little change. The middle melting peak increases with T_c but with a lesser slope than the lowest melting peak. Above T_c = 500 K, only one melting peak is left (Figure 9), and it increases with T_c and becomes increasingly sharper. Extrapolation of the peak temperature T_m(p) with respect to T_c reaches the line of $T_m = T_c$ at about 610 K, as a first guess at an equilibrium melting temperature of PEN. The results of this extrapolation are shown in Figure 11. Crystallization from the glass (see Figure 10) leads again to three melting peaks of similarity to Figure 8. Differences arise only for the middle melting peak.

Heat of Fusion of PEN. On the basis of setting of the base line by heat capacity data, Figures 8–10 can be used for quantitative analysis of the heat of fusion. Additional melting traces of T_c in the 500–520 K region crystallized

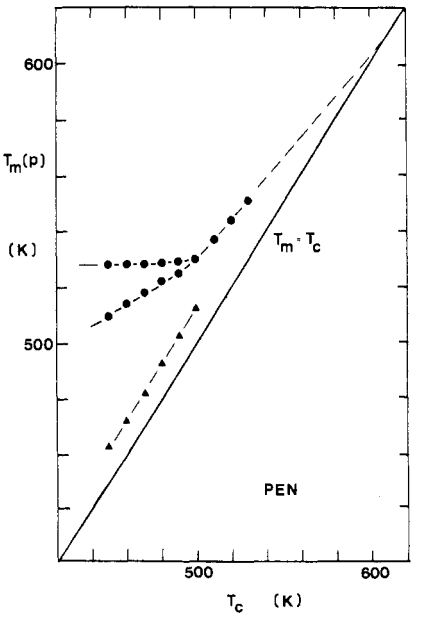

Figure 11. Relationship between T_m and T_c of PEN. The solid line is for $T_c = T_m$. Below T_c = 500 K three melting peaks are observed; above 500 K only one peak is left (see text).

Table II
Thermal Properties of PEN in the Melting Transition Region Measured on Heating at 10 K/min

T_c and t_c	w^c(T)	w^c(H)	w^c(M)	w^c(L)	w^c(I)	w^c(C)	$f_r - w^c$(T)
A. Isothermal Crystallization from the Melt and Then Cooling at 10 K/min							
450 K, 2 h	0.30	0.265	0.005	0.03	0.30	0.00	0.19
460 K, 1.5 h	0.33	0.25	0.04	0.03	0.32	0.01	0.17
470 K, 1 h	0.36	0.24	0.08	0.03	0.35	0.01	0.15
480 K, 0.5 h	0.39	0.21	0.13	0.04	0.38	0.01	0.12
490 K, 1 h	0.44	0.20	0.18	0.05	0.43	0.01	0.10
495 K, 1.5 h	0.45	0.23	0.21		0.44	0.01	0.06
500 K, 2 h	0.48	0.24	0.22		0.46	0.02	0.03
510 K, 4 h	0.49	0.47			0.47	0.02	0.00
520 K, 15 h	0.51	0.48			0.48	0.03	0.00
B. Isothermal Crystallization from the Glass and Then Cooling at 10 K/min							
450 K, 2 h	0.28	0.24	0.005	0.03	0.275	0.005	0.21
460 K, 1.5 h	0.32	0.25	0.03	0.03	0.31	0.01	0.18
470 K, 1 h	0.35	0.23	0.08	0.03	0.34	0.01	0.16
480 K, 0.5 h	0.38	0.20	0.13	0.04	0.37	0.01	0.14
490 K, 1 h	0.42	0.15	0.20	0.06	0.41	0.01	0.11
495 K, 1.5 h	0.43	0.17	0.24		0.41	0.02	0.07
500 K, 2 h	0.45	0.18	0.25		0.43	0.02	0.04
510 K, 4 h	0.47	0.45			0.45	0.02	0.00
520 K, 15 h	0.50	0.47			0.47	0.03	0.00

from the glass are practically the same as those from the melt shown in Figure 9 and are not separately shown. All results are listed in Table II. There are four parts to the heat of fusion below T_c = 490 K: (1) that of the high-temperature melting peak, (2) that of the middle-temperature melting peak, (3) that of the low-temperature melting peak, and (4) that set during the cooling at 10 K/min from T_c to room temperature. The last part can be determined by difference from the samples analyzed with and without cooling before analysis. This latter heat of fusion is usually less than 2% of the total heat of fusion in contrast to prior experiments done with PEEK where w^c(C) could be as much as 13%.[9] The reason seems to be the much slower crystallization of PEN at the lower temperature (see also Figure 1). Above T_c = 490 K, the melting peaks start to merge. At T_c = 500 K, two melting peaks can be distinguished, but only one melting peak can be observed above T_c = 500 K.

For the isothermal crystallization from the melt below 490 K one finds that the total crystallinity, w^c(T), increases only based on the contribution of w^c(M), the crystallinity of the middle melting peak (from 0.005 to 0.18). In the narrow temperature range between 490 and 500 K the melting behavior seems to undergo a large change. Above T_c = 500 K only one melting peak can be observed, namely, w^c(H), and it increases continuously with increasing T_c. The crystallinity gained during cooling from T_c is also slightly increased (0.01–0.03).

Finally, a comparison between the rigid fraction from ΔC_p at T_g, f_r (eq 1), shown in Table I and the total crystallinity, w^c(T) (eq 2), has been made. The data are listed also in Table II ($f_r - w^c$). $f_r - w^c$ can be called, as before, the rigid-amorphous fraction. One can find that the rigid-amorphous fraction is high at low crystallization temperatures (0.19 for crystallization from the melt and 0.21 for crystallization from the glass at T_c = 450 K). It decreases with increasing T_c, and above 500 K no rigid-amorphous fraction can be observed within our experimental error. In general, the rigid-amorphous fraction in the glass crystallization is a few percent higher than in the melt crystallization at the same T_c.

The heat of fusion of 100% crystalline PEN is estimated to be 25 ± 2 kJ/mol. A detailed procedure of determining ΔH_f of 100% crystalline PEN will be described elsewhere.[18]

Reorganization during Fusion. In order to study the changes in the melting peaks, we have used different heating rates for analysis after isothermal crystallization

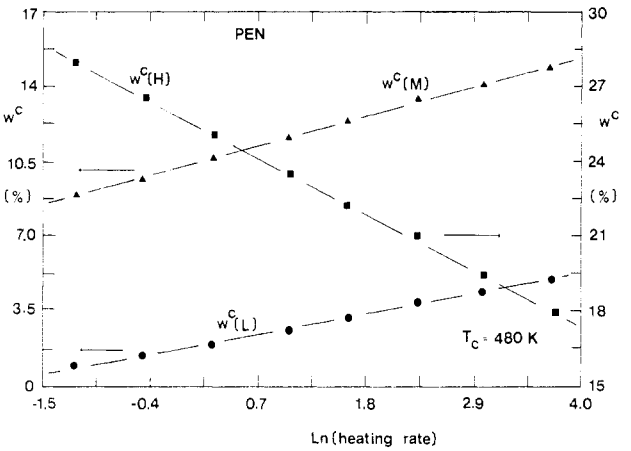

Figure 12. Relationship between three crystallinities, w^c(L), w^c(M), and w^c(H) and logarithm of the heating rate (in K/min). Samples crystallized at 480 K from the melt for 0.5 h.

without cooling. The results of samples crystallized at 480 K are shown in Figure 12 as an example. One can find that at T_c = 480 K for three melting peaks the crystallinity of the lower melting peak, w^c(L), and that of the middle melting peak, w^c(M), increase with heating rate. Correspondingly, the crystallinity of the higher melting peak, w^c(H), decreases, so that the total crystallinity obtained during the isothermal crystallization is not changed. Similar observations were made for the other crystallization temperatures below 500 K. The samples thus have before analysis at low temperatures considerably higher w^c(L) and w^c(M) and much lower w^c(H). On heating, crystal perfection, in addition, shifts the melting temperatures, as is also obvious from Figure 11.

Melting of Samples after Two-Step Isothermal Crystallization. Figures 13–15 show DSC melting traces for the two-step isothermal crystallizations and the corresponding single-step crystallization. Superficially the two-step crystallization corresponds to the normal (one-step) isothermal crystallizations. One can find, from Figures 13 and 14, that there is some "memory effect" in the middle and upper melting peaks similar to other polymers containing phenylene groups.[9,11] Namely, the higher melting peak temperatures for the two-step isothermal crystallization are fixed at the first step of the crystallization. The lower melting peak changes or disappears following the second crystallization step. The

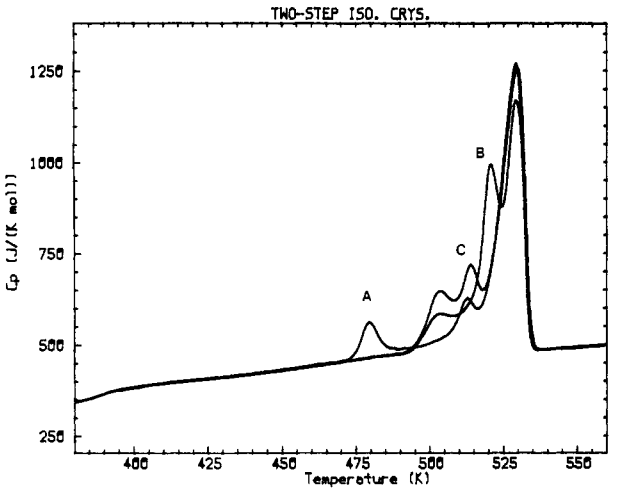

Figure 13. Two-step isothermal crystallization from the glass: A, T_c = 470 K, held 1 h, one-step isothermal crystallization (see Table II); B, T_c = 490 K, held 1 h, one-step isothermal crystallization (see Table II); C, two-step isothermal crystallization, T_c = 470 K, held 1 h, heated to 490 K at 10 K/min, held 1 h, cooled to 330 K with 10 K/min before recording.

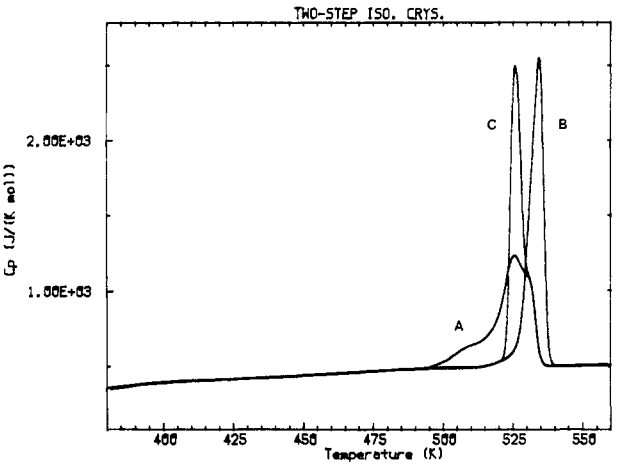

Figure 14. Two-step isothermal crystallization from the melt: A, T_c = 490 K, held 1 h, one-step isothermal crystallization (see Table II); B; T_c = 510 K, held 4 h, one-step isothermal crystallization, (see Table II); C, two-step isothermal crystallization, T_c = 490 K, held 1 h, heated to 510 K at 10 K/min, held 4 h, coold to 330 K with 10 K/min before recording.

"memory effect" is changed as soon as only one melting peak exists, as is shown in Figure 15. Two-step crystallization produces a crystal distribution melting at an intermediate temperature.

Sequence of Crystallization. To establish the sequence of crystallization of PEN, isothermal crystallization at 500 K was performed and interrupted at different crystallization times. Figure 16 shows the immediate analysis after different times, t_c. After 1.5 min there is still no observable crystallization so that this run could be taken as a base line. With increasing t_c, development of the crystallinity leading to the high melting peak, w^c(H), can be observed. The lower melting peak, w^c(M) (as listed in Table II), becomes distinct after 15 min. At higher t_c the ratio of w^c(M) to w^c(H) increases with time. The higher peak moves to slightly higher melting temperature as crystallization proceeds. The lower melting peak increases also, from 511 K at t_c = 15 min to 520 K at t_c = 120 min.

Discussion

Heat Capacity below T_g. Below 300 K the heat capacity of all 23 samples with different crystallinities and

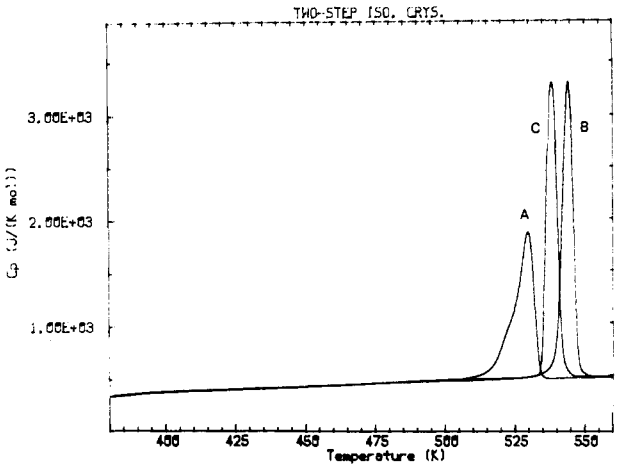

Figure 15. Two-step isothermal crystallization from the melt: A, T_c = 500 K, held 2 h, one-step isothermal crystallization (see Table II); B, T_c = 520 K, held 15 h, one-step isothermal crystallization (see Table II); C, two-step isothermal crystallization, T_c = 500 K, held 2 h, heated to 520 K at 10 K/min, held 15 h, cooled to 330 K with 10 K/min before recording.

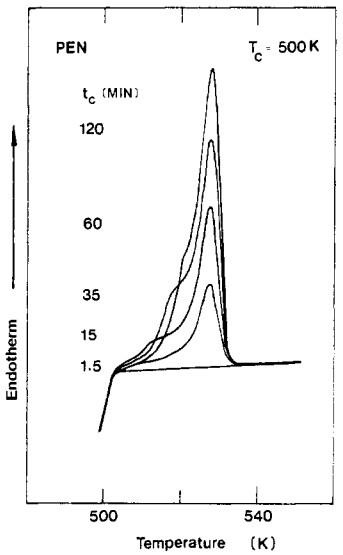

Figure 16. Analysis of crystals grown at 500 K for different lengths of time. The flat line after 1.5-min crystallization shows no crystallization.

the totally amorphous samples agreed within experimental error. Such independence of C_p on rigid fraction (or crystallinity) has been widely observed for other polymers.[19]

Above 300 K, there is a slight dependence of C_p on rigid fraction (or crystallinity). A cause of such pre-glass transition behavior may be local modes of motion[20] that are still active below T_g. It has been reported that the naphthalene group in the backbone chain of macromolecules starts to have a local motion at about 323 K, demonstrated experimentally by dielectric and mechanical measurements.[21]

On the basis of the solid and liquid heat capacity data, the heat capacity increase at T_g is 80.1 J/(K mol) which involves the pre-glass transition-like contribution [9.5 J/(K mol)]. This value is in agreement with the empirical rules of increase in heat capacity at T_g [11.3 J/(K mol bead)][22] if one considers that there are four small beads in PEN in addition to the naphthalene group that may contribute as much as three small beads [34 J/(K mol bead)].

Hysteresis in the T_g Region. Figure 3 shows that amorphous PEN has a typical hysteresis in heat capacity.[23] As long as the cooling rate is slower than 2.5 K/min, the

hysteresis effect of PEN is similar to that observed for other polymers; i.e., a linear relationship exists between Δh of the hysteresis peak and the logarithm of the cooling rate and $\Delta h = 0$ being extrapolated to the condition that heating and cooling rates are about equal (10 K/min).

The positive deviation from the linear relationship in Figure 4 indicates, however, that the freezing and unfreezing of motion of PEN at the glass transition temperature is asymmetric. Similar situations have been observed in PPO[10] and PC[24] cases. On the other hand, for PEEK[9] and PPS,[11] one could not find such positive deviation down to the cooling rate of 10 K/min. The deviation from linearity must be connected to the annealing kinetics of the glass. Polymer chains with a backbone width larger than that of the phenylene group (0.5 nm) seem to often cause such positive deviation.

Semicrystalline PEN samples do in most cases show no hysteresis. The broadening of the glass transition region (Table I) is not sufficient to explain the disappearing of hysteresis. The interaction between crystal and amorphous phase must thus reduce the time dependence of the glass transition, as was found recently for other semicrystalline polymers, such as PET.[25]

Figure 5 indicates that there is a linear relationship between the glass transition temperature of amorphous PEN and the logarithm of cooling rate. Not suprisingly, it is a common feature of the glass transition region for macromolecules. Similar relationships were established earlier for polystyrene[23] and poly(methyl methacrylate).[26]

Glass Transition of Semicrystalline PEN. Figures 1 and 3 show that quenched PEN has the sharpest glass transition. The observed ΔC_p of 80.1 J/(K mol) [9.5 J/(K mol) for pre-glass transition included] can also be used to calculate the rigid fraction of semicrystalline PEN based on eq 1. Any crystallization broadens the glass transition range and shifts its end, T_e, to higher temperatures by as much as 30 K. For the isothermal crystallization below T_c = 490 K, one can find that the glass transition temperature, T_g, is shifted to a higher temperature as the crystallization becomes more restrictive. Above T_c = 490 K, an almost constant glass transition can be observed (see Table I and Figure 6). Only T_e decreases continuously with increasing T_c. Surprisingly, the constant T_g is also close to the T_g of amorphous PEN cooled at a rate of 10 K/min (see Figure 3). Coupled to the broadening of the glass transition and increase of T_g below T_c = 490 K is also the increase of the rigid-amorphous fraction of PEN (Table II). For T_c = 450 K, e.g., the rigid-amorphous portion of the polymer reaches about 27–29% of the remaining amorphous portion (70–72%, crystallinity 28–30%). Above T_c = 500 K, there is no rigid-amorphous fraction, which seems to be linked also to a constant T_g. The rigid-amorphous fraction disappears as soon as the lowest melting peak is reached (see below).

Combining all these facts, below T_c = 490 K, there is a broadening of the glass transition region, a shift of T_g to higher temperature, and an increase of the rigid-amorphous fraction with decreasing T_c. In addition, this is also the temperature region where multiple melting peaks are observed. Above T_c = 490 K, there is a constant T_g which is almost the same as for amorphous PEN and only one melting peak in the DSC traces. This leads to the deduction that the rigid-amorphous fraction and the change in T_g are due to the existence of defect crystals of lower melting peak temperature.

According to Figure 7 the rigid-amorphous state starts to become mobile above 430 K, somewhat below the lowest melting peak of 450 K. However, total mobility must await full perfection of the low melting crystals.

Melting Behavior of PEN. The melting behavior of PEN is strongly dependent on the crystallization history, as shown in Figure 11. At lower crystallization temperature, three melting peaks can be observed (Figures 8 and 10). Four different crystallinities must thus be identified: (1) the high-melting and usually major portion, w^c(H); (2) the middle-melting portion, w^c(M); (3) the low-melting portion, w^c(L); and (4) a broad portion crystallized on cooling, w^c(C). With increasing T_c, as shown in Figure 9, two melting peaks and finally only one peak are left.

Table II has a list of all those crystallinity data. For both isothermal crystallization from the melt and glassy states, the total crystallization, w^c(T), and the isothermally grown crystallinity, w^c(I), increase continuously with T_c. The discussion of the other partial crystallinities must take into account the heating rates, as shown in Figure 12. Although it may be possible to eliminate w^c(L) by slow heating, the data in Figure 16 reveal that annealing to high melting w^c(H) is already far advanced during the isothermal crystallization.

The two-step crystallizations (Figures 13–15) show that the perfection of the low-melting crystals on heating to the middle-melting crystals or the middle ones to the high-melting crystals is restricted by the already present low-temperature-grown high-melting crystals. To anneal an imperfect crystal at a given temperature under these conditions is more difficult than to grow a new crystal at the same temperature.

The T_m/T_c plot (Figure 11) shows the typical polymer behavior. The low-melting peak is similar to the "annealing peak",[12] and the high melting peak stays constant for a wide crystallization temperature due to the crystal perfection on heating. The middle melting peak increases with T_c but disappears as soon as T_c = 500 K.

The additional crystallinity developed on cooling after completion of crystal growth at T_c, w^c(C) is usually small because of the slow crystallization of PEN. It must represent crystals of low perfection and may be closely linked to the formation of the rigid-amorphous fraction.

Conclusions

In thermal analysis of PEN it is necessary to determine the rigid-amorphous fraction. Such characterization can be carried out only after determination of the solid and liquid heat capacity base lines. In the glass transition region, information on the breadth and hysteresis of the glass transition is valuable in addition to T_g and ΔC_p information. Four specific crystallinities are identified: w^c(H), w^c(M), w^c(L), and w^c(C). All of the crystals and the rigid-amorphous fraction are metastable, and their change during analysis due to reorganization, perfection, and recrystallization must be assessed.

To fully understand the rigid-amorphous state, one needs to further study molecular motion in the solid state.

Acknowledgment. This work was supported by the National Science Foundation, Polymers Program, Grant No. DMR 83-17097.

Registry No. PEN (copolymer), 25230-87-9; PEN (SRU), 24968-11-4.

References and Notes

(1) Bell, V. L.; Pezdirtz, G. F. *J. Polym. Sci., Polym. Chem. Ed.* **1983**, *21*, 3083. See also: Allen, N. S.; McKeller, J. F. *J. Appl. Polym. Sci.* **1978**, *22*, 2085.
(2) Richards, R. R.; Rogowski, R. S. *J. Polym. Sci., Polym. Phys. Ed.* **1974**, *12*, 89.
(3) Jackson, W. J., Jr. *Macromolecules* **1983**, *16*, 1027.
(4) Mencik, Z. *Chem. Prum.* **1967**, *17*, 78.
(5) Desai, A. B.; Wilkes, G. L. *J. Polym. Sci., Symp.* **1974**, *46*, 291.

(6) Makarewicz, P. J.; Wilkes, G. L. *J. Appl. Polym. Sci.* **1978**, *22*, 3347.
(7) Ouchi, I.; Hosoi, M.; Shimotsuma, S. *J. Appl. Polym. Sci.* **1977**, *21*, 3456.
(8) Gaur, U.; Wunderlich, B. *Macromolecules* **1980**, *13*, 445.
(9) Cheng, S. Z. D.; Cao, M.-Y.; Wunderlich, B. *Macromolecules* **1986**, *19*, 1868.
(10) Cheng, S. Z. D.; Wunderlich, B. *Macromolecules* **1987**, *20*, 1630.
(11) Cheng, S. Z. D.; Wu, Z. Q.; Wunderlich, B. *Macromolecules* **1987**, *20*, 2082.
(12) Wunderlich, B. *Macromolecular Physics, Crystal Melting*; Academic: New York, 1980; Vol. III.
(13) Wunderlich, B.; Bopp, R. C. *J. Thermal Anal.* **1974**, *6*, 335. See Also: Mehta, A.; Bopp, R. C.; Gaur, U.; Wunderlich, B. *J. Thermal Anal.* **1978**, *13*, 197.
(14) Ginnings, D. C.; Furukawa, G. T. *J. Am. Chem. Soc.* **1953**, *75*, 522.
(15) Cheng, S. Z. D.; Wunderlich, B. *J. Polym. Sci., Polym. Phys. Ed.* **1986**, *24*, 577, 595.
(16) Bu, H. S.; Cheng, S. Z. D.; Wunderlich, B., in preparation.
(17) Cheng, S. Z. D.; Bu, H. S.; Pan, R.; Wunderlich, B., to be submitted for publication in *Makromol. Chem.*
(18) Cheng, S. Z. D.; Wunderlich, B.; Wu, Z. Q.; Li, W. H., in preparation.
(19) See, for example: Wunderlich, B.; Baur, H. *Adv. Polym. Sci.* **1970**, *7*, 151.
(20) Ferry, J. D. *Viscoelastic Properties of Polymers*, 3rd ed.; Wiley: New York, 1980.
(21) Blundell, D. J.; Buckingham, K. A. *Polymer* **1985**, *26*, 1623.
(22) Wunderlich, B. *J. Phys. Chem.* **1960**, *64*, 1052. Gaur, U.; Wunderlich, B. *Polym. Prpr. (Am. Chem. Soc., Div. Polym. Chem.)* **1979**, *20*, 429.
(23) Wunderlich, B.; Bodily, D. M.; Kaplan, M. H. *J. Appl. Phys.* **1964**, *35*, 95.
(24) Unpublished observation in our ATHAS Laboratory.
(25) Menczel, J.; Wunderlich, B. *J. Polym. Sci., Polym. Lett. Ed.* **1981**, *19*, 261.
(26) Wolpert, S. M.; Weitz, A.; Wunderlich, B. *J. Polym. Sci., Polym. Phys. Ed.* **1971**, *9*, 1887.

On the Curing Theory and the Scaling Study of the Polycondensation Reaction of $A_{a_1}...A_{a_s}$–$B_{b_1}...B_{b_t}$ Type

Tang Au-chin, Li Ze-sheng, Sun Chia-chung, and Tang Xin-yi*

Institute of Theoretical Chemistry and Department of Chemistry, Jilin University, Changchun, China. *Received May 14, 1987; Revised Manuscript Received August 28, 1987*

ABSTRACT: For the polycondensation reaction of $A_{a_1}...A_{a_s}$–$B_{b_1}...B_{b_t}$ type, the sol fraction above the gel point is investigated in detail by taking Stockmayer's gelation condition as a criterion. Furthermore, the scaling behavior near the gel point is revealed to reach an asymptopic form of Stockmayer's equilibrium number distribution from which a generalized scaling law is deduced.

Introduction

As is well-known, the polycondensation reaction of $A_{a_1}...A_{a_s}$–$B_{b_1}...B_{b_t}$ type has been initiated by Stockmayer.[1-5] In this paper, above the gel point, which is regarded as the threshold of the sol–gel transision,[3,5-10] the behavior of the sol fraction involving the total, sol, and gel equilibrium fractional conversions is investigated in detail by taking Stockmayer's gelation condition[3] as a criterion. With limitation of procedure approached from above the gel point, three equivalent forms of the gel point are obtained.

It is known that in the theory of branching processes, the probability generating function with differentiation technique proposed by Gordon[8,11] can be used for evaluation of polymer moments. In this paper, based on Stockmayer's equilibrium number distribution of $A_{a_1}...A_{a_s}$–$B_{b_1}...B_{b_t}$ type,[3] a direct differentiation method with some mathematical techniques is presented to obtain the recursion formula of polymer moments in the form

$$M_{k+1} = D\left[EM_k + Fp_a\left[(1-p_a)\frac{\partial M_k}{\partial p_a} + \partial_x M_k \right] + Ip_b\left[(1-p_b)\frac{\partial M_k}{\partial p_b} + \partial_y M_k \right] \right] \quad (1)$$

This formula is suitable for both above and below the gel point, and especially, it is useful in approaching the scaling study near the gel point.[12-14]

For revealing the critical behavior of a sol–gel transition, a reasonable approach without using the Stirling approximation[12] is proposed to reach an asymptopic form of Stockmayer's equilibrium number distribution

$$\tilde{P}(n_1,...,n_s,l_1,...l_t) = B(s+t-1)!(n_1+...+n_s+l_1+...+l_t)^{-(s+t+(3/2))} \times \exp\left[-\left(k-\frac{3}{2}\right)\frac{(n_1+...+n_s+l_1+...+l_t)}{n\xi(k)} \right] \quad (2)$$

with

$$\tilde{P}_n = \int_0^n dm_{s+t-1} \int_0^{m_{s+t-1}} dm_{s+t-2} ... \int_0^{m_2} dm_1 \times \tilde{P}(m_1, m_2 - m_1, ..., m_{s+t-1} - m_{s+t-2}, n - m_{s+t-1})$$

$$\tilde{P}_n = Bn^{-5/2} \exp\left[-\left(k-\frac{3}{2}\right)\frac{n}{n\xi(k)} \right] \quad (3)$$

where B is a normalization constant

$$B = (2\pi J)^{-1/2} E(p_a^c, p_b^c) \quad (4)$$

and where the generalized typical size[14] $n\xi(k)$ is defined as

$$n\xi(k) = (p_b^c/2)^2(2k-3)J|p_b - p_b^c|^{-2} \quad (5)$$

Consequently, a generalized scaling law[13,14]

$$\tau - 2 = \sigma\beta \quad (6)$$

$$k + 1 - \tau = \sigma\gamma_k \qquad k = 2, 3, ... \quad (7)$$

is deduced.

Sol Fraction above the Gel Point with Stockmayer's Gelation Condition as a Criterion

Let us consider a polycondensation system consisting of two species of monomers A_{a_i} and B_{b_j} with functionalities

0024-9297/88/2221-0797$01.50/0